Bioorganic Chemistry 86 (2019) 550–556

Contents lists available at ScienceDirect

Bioorganic Chemistry

journal homepage: www.elsevier.com/locate/bioorg

Oxidative functionalization of a halimane diterpenoid achieved by fungal transformation

Afif Felix Monteiro[a,1,*], Gabriela Marinho Righetto[b], Laura Vilar Simões[a], Larissa Costa de Almeida[c], Letícia Veras Costa-Lotufo[c], Ilana Lopes Baratella da Cunha Camargo[b], Ian Castro-Gamboa[a,*]

[a] Núcleo de Bioensaios, Biossíntese e Ecofisiologia de Produtos Naturais (NuBBE), Universidade Estadual Paulista (UNESP), Instituto de Química, Departamento de Química Orgância, Francisco Degni, 55, 14800-900, Araraquara, SP, Brazil
[b] São Carlos Institute of Physics, University of São Paulo, PO Box 369, 135560-970, São Carlos, SP, Brazil
[c] Universidade de São Paulo (USP), Instituto de Ciências Biomédicas, Av. Lineu Prestes, 1524, 05508-900, São Paulo, SP, Brazil

ARTICLE INFO

Keywords:
Microbial transformation
Halimane diterpenoid
C−H oxidation
Double-bond hydration
Biofilm reduction

ABSTRACT

Regio and stereoselective activation of sp^3 C−H bonds remain one of the major advantages of biocatalysis over traditional chemocatalytic methods. Herein, we describe the oxy-functionalization of halimane diterpenoid **1** by whole cells of three filamentous fungi, aiming to obtain derivatives with desirable biological properties. After incubating **1** with *Fusarium oxysporum*, *Myrothecium verrucaria*, and *Rhinocladiella similis* at different concentrations and incubation times, four known (**3**, **5**, **6**, and **7**) and three new (**2**, **4**, and **8**) halimane derivatives were obtained and characterized. *F. oxysporum* catalyzed the hydroxylation of positions C-2 (**2**) and C-7 (**4**), while *R. similis* simultaneously mediated the 2-oxo-functionalization and the hydration of 13,14-(C−C)double bond belonging to an *α,β*-unsaturated carbonyl system (**8**). Compounds **1–7** were non-cytotoxic against HCT-116 and MCF-7 cancer cell lines at tested concentrations. However, substrate **1** displayed moderate reduction ability against biofilm produced by *Staphylococcus epidermidis* ATCC35984 (84% at 1.6 mM), and this effect was retained to some extent by derivatives **4** and **7**. These results emphasize the prominent potential of filamentous fungi associated with the microbiota of medicinal plants as versatile catalysts for singularly useful reactions through their complex enzymatic machinery, as well as the high susceptibility of halimane-diterpenoid substrates.

1. Introduction

Regardless of the remarkable achievements in synthetic organic chemistry reached during the last years, one of the major challenges that still remains is the regio and stereoselective oxidative activation (hydroxylation) of sp^3 C−H bonds of organic compounds. These reactions are often difficult or impossible to achieve even using state-of-the-art of transition metal catalysts or organocatalysts [1]. In fact, C−H bonds are highly stable and with the simultaneous availability of several similarly reactive sites for activation even in a simple molecule, the discrimination among unactivated positions in the absence of strong directing effects is still completely out of the scope of current chemocatalytic methods [2,3]. As an alternative approach, biocatalysis has been proven to be potentially advantageous over traditionally synthetic means in the last decades, especially regarding the selective oxy-functionalization of unactivated sp^3 C−H bonds [4,5]. Selectivity is normally reached because of the large contact surface between the enzyme and its substrate, as only one site (regiocontrol) and face (stereocontrol) of the substrate is properly positioned into the catalytic machinery [6]. Biocatalytic processes are usually categorized into biotransformations and fermentation reactions. Biotransformations can be catalyzed either by isolated enzymes or by microbial-whole cells, in which a cheap organic source is employed for catalyst production and an additional substrate is converted into a product through single or multistep catalysis [4]. Fungal whole-cell transformation is an effective approach to achieve chemical modifications from a variety of starting materials, such as bioactive natural products or synthetic compounds in order to reach chemical diversity and possibly enhanced or improved biological properties [7].

Diterpenoids constitute a chemically heterogeneous class of

* Corresponding authors.
E-mail addresses: afif.afm@gmail.com (A.F. Monteiro), ian.castro@unesp.br (I. Castro-Gamboa).
[1] Instituto de Química de São Carlos, Universidade de São Paulo, CP 780, CEP 13560-970, São Carlos, SP, Brazil.

https://doi.org/10.1016/j.bioorg.2019.02.021
Received 30 November 2018; Received in revised form 7 February 2019; Accepted 8 February 2019
Available online 11 February 2019
0045-2068/

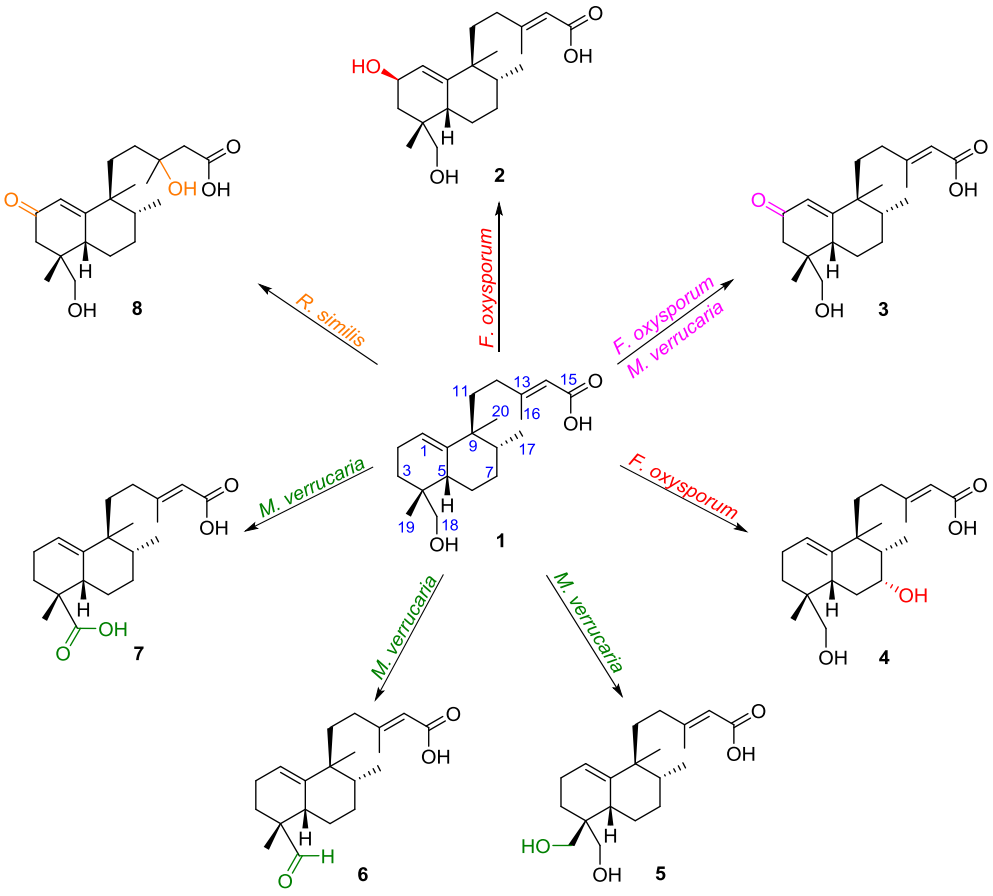

Fig. 1. Biotransformation products obtained from substrate **1** with *F. oxysporum*, *M. verrucaria,* and *R. similis*.

secondary metabolites, possessing a C_{20} carbon skeleton based on four isoprenoid units [8], exhibiting a decalin core and a C_6-side chain [7] and comprise the largest family of molecules among terpenoids, encompassing > 18,000 compounds. They display extensive chemodiversity correlated with a wide range of biological properties [9]. Halimane diterpenoids can be biogenetically considered as derived from labdanes by rearrangement involving hydride(s) and methyl group migration (C-20 from C-10 to C-9 position), leading to $\Delta^{1(10)}$, $\Delta^{5(10)}$, or Δ^5 halimanes. These chemotypes can be found in different plant species from several families and in other taxonomic groups, such as marine organisms and microorganisms [9].

In a previous report[7], we investigated the biotransformation of the halimane diterpenoid substrate **1** (Fig. 1) by two filamentous fungi strains, *Fusarium oxysporum*, and *Myrothecium verrucaria*, respectively isolated from the rhizosphere and from the aerial parts of the plant *Senna spectabilis* (Fabaceae) [10]. These experiments afforded four oxidized derivatives which were assayed for anticholinesterase activity [7,11]. As a continuation of our work on the biotransformation ability of filamentous fungi towards natural diterpenoid substrates, we report the influence of incubation time and substrate concentration on whole-cell fungal transformation of seven oxy-functionalized products, including four known (**3**, **5**, **6**, and **7**) and three new (**2**, **4**, and **8**) derivatives. In addition, the substrate and its products were assessed for cytotoxic, antibacterial and biofilm reduction activities.

2. Results and discussion

2.1. Structure elucidation of biotransformation products

Incubation of substrate **1** with *F. oxysporum* allowed the isolation of the three biotransformation products **2**, **3**, and **4** (Fig. 1), while substrate oxidation by *M. verrucaria* led to four metabolites, including bioproduct **3** and three other compounds (**5**, **6**, and **7** – Fig. 1). Finally, fungal transformation with *R. similis* provided one additional derivative **8** (Fig. 1).

The structure elucidation of the oxidation products was accomplished by combining the information from 1D (^{1}H, ^{13}C, DEPT-135, NOESY, and TOCSY) and 2D (HSQC and HMBC) NMR experiments, and confirmed by HRESIMS data, as well as by literature data comparison.

Compound **3** was identified as the 2-oxo substrate analogue previously obtained by *F. oxysporum* [7], which is reported for the first time from incubation with *M. verrucaria*. Metabolites **5**, **6**, and **7** were identified, respectively, as the oxidized series of natural derivatives 18,19-dihydroxy (**5**), 18-formyl (**6**), and 18-carboxy (**7**) previously produced through substrate-transformation catalyzed by *M. verrucaria* [7]. Products **2** and **4** formed by substrate conversion with *F. oxysporum*, as well as compound **8** which was obtained by feeding of *R. similis*, had their structures determined and to the best of our knowledge, they correspond to new compounds not described so far.

Compound **2** (Fig. 1) was isolated as a white, amorphous solid, and its molecular formula was determined to be $C_{20}H_{32}O_4$ according to its HRESIMS spectrum, which revealed an ion peak at *m/z* 335.2233 $[M-H]^-$ (calcd. for $C_{20}H_{31}O_4$, 335.2228) corresponding to the deprotonated molecule, suggesting the insertion of an oxygen atom (hydroxylation) to the substrate ($C_{20}H_{32}O_3$) by *F. oxysporum*. The ^{1}H NMR spectrum showed the presence of a signal at δ_H 4.32 (dd, J = 5.0; 6.0 Hz), arising from a new oxymethine hydrogen, assigned to the carbon showing a chemical shift (δ_C) 72.2 ppm through direct ^{1}H-^{13}C correlation observed in the HSQC spectrum. Therefore, the position of the hydroxylation occurrence was established at C-2 via the inspection of long-range correlations of the HMBC spectrum, which demonstrated a cross-peak between the signal attributed to H-1 (δ_H 5.68) and that of

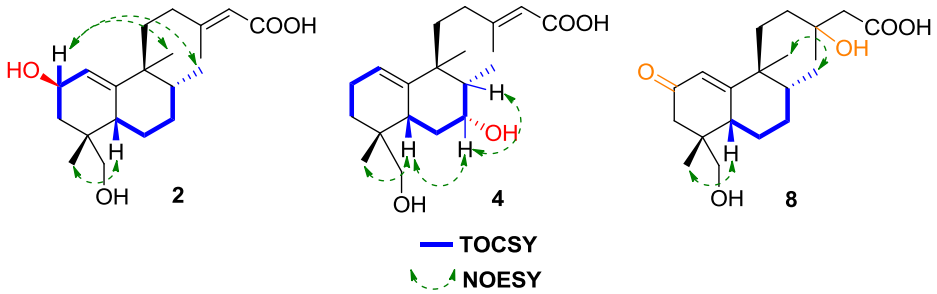

Fig. 2. Key NOESY and TOCSY correlations for compounds **2**, **4**, and **8**.

Table 1
^{1}H (600.13 MHz) and ^{13}C NMR (150.9 MHz) spectroscopic data for compounds **2** ($CDCl_3$), **4** and **8** (CD_3OD).

Position	2		4		8	
	δ_C	δ_H (*J* in Hz)	δ_C	δ_H (*J* in Hz)	δ_C	δ_H (*J* in Hz)
1	124.6	5.68, *dd* (1.8; 6.0)	122.9	5.46, *t* (3.5; 1.1)	125.0	5.79, *s*
2	72.2	4.32, *dd* (5.0; 6.0)	23.4	2.09, *m*	201.8	
3	44.4	1.80, *m* 1.66, *m*	28.1	1.10, *dt* (4.5; 9.1) 1.37, *m*	43.5	2.35, *d* (16.0) 1.92, *d* (16.0)
4	43.0		37.1		39.9	
5	47.1	2.28, *ddt* (1.9; 3.7; 5.1; 6.2)	40.2	1.96, *m*	43.8	2.48, *dd* (4.4; 12.9)
6	20.4	1.63, *m* 1.50, *m*	32.4	1.81, *m* 1.21, *m*	25.5	1.93, *m* 1.60, *ddd* (4.4; 12.6; 17.0)
7	27.7	2.00, *m* 1.43, *m*	69.5	4.26, *dt* (4.7; 9.3)	29.7	2.19, *m* 1.42, *m*
8	38.1	1.62, *m*	46.6	1.71, *m*	43.0	1.86, *m*
9	41.9		44.7		46.4	
10	145.2		140.6		173.9	
11	36.7	1.84, *m*; 1.36, *td* (4.8; 12.8)	38.1	2.06, *m* 1.35, *m*	34.4	2.27, *m* 1.38, *m*
12	36.2	2.01, *m*; 1.76, *m*	36.9	2.10, *m* 1.83, *m*	37.6	1.49, *m*
13	164.3		162.6		72.1	
14	114.6	5.67, *dd* (1.3; 2.2)	116.6	5.63, *sl*	48.3	2.26, *m* 2.23, *m*
15	170.4		170.3		174.0	
16	19.7	2.16, *d* (1.3)	19.1	2.12, *d* (1.1)	27.2	1.18, *s*
17	15.9	0.88, *d* (7.0)	8.0	0.75, *d* (6.9)	15.9	0.85, *d* (7.1)
18	72.8	4.03, *d* (8.5) 3.36, *dd* (1.7; 8.5)	69.6	3.44, *d* (10.7) 3.28, *d* (10.7)	69.1	3.53, *d* (11.0) 3.51, *d* (11.0)
19	22.4	1.16, *s*	22.6	0.98, *s*	23.4	1.04, *s*
20	22.6	0.93, *s*	22.9	1.01, *s*	21.7	1.03, *s*

δ_C 72.2 (C-2). Moreover, a comparative analysis between the ^{13}C NMR data from the biotransformation product **2** with that of the starting compound (**1**) [7] provided evidence of *β*-effects at C-1 (+4.5) and C-2 (+17.9), reinforcing the assignments. The position of the new group at C-2 was further supported by 1D TOCSY experiments, through the selective irradiation of the H-2 signal (δ_H 4.32), which confirmed the connectivity among the groups constituting the spin system (CH-1)-(CH-2)-(CH_2-3) (Fig. 2). The spatial orientation of the new hydroxyl group was inferred from the information provided by a 1D NOESY spectrum, which showed correlations among the signals at δ_H 4.32 (H-2) with δ_H 1.16 (CH_3-19), and δ_H 0.93 (CH_3-20), indicating that these groups are co-facially oriented (face *α*) and, consequently, the 2-OH group is *β*-disposed. The relative configurations of the stereogenic centers deduced from the key NOE correlations are shown in Fig. 2 and its complete ^{1}H and ^{13}C NMR data assignments are compiled at Table 1.

Natural derivative **4** (purified as a white, amorphous powder) had the molecular formula $C_{20}H_{32}O_4$, deduced from its HRESIMS spectrum, referring to the deprotonated molecule ion at *m/z* 335.2233 $[M\text{-}H]^-$ (calcd. for $C_{20}H_{31}O_4$, 335.2228), indicating the incorporation of an oxygen atom (hydroxylation) to the substrate. The appearance of a signal at δ_H 4.26 (dt, J = 4.7; 9.3 Hz), characteristic of the resonance of a new oxymethine group, was observed in the ^{1}H NMR spectrum. The ^{13}C and DEPT-135 NMR spectra showed a signal at δ_C 69.5, corroborating the presence of an additional oxymethyne. These signals (δ_H 4.26 and δ_C 69.5) were observed to be correlated in the HSQC spectrum, and the position of the new hydroxyl group was defined as C-7 through HMBC correlations verified among the signals corresponding to H-8 (δ_H 1.71) and H_2-6 (δ_H 1.81; 1.21) with δ_C 69.5 (C-7). Additional evidence was given by *β*-effects for C-8 (+5.5) and C-6 (+7.2), which are consistent with this proposal. Irradiation at the frequencies of the signals attributable to H-3b (δ_H 1.10, *dt*, J = 4.5; 9.1 Hz) and H-1 (δ_H 5.46, *t*, J = 1.1; 3.5 Hz) through 1D TOCSY experiment allowed observation of the ^{1}H-^{1}H correlations of the (CH-1)-(CH_2-2)-(CH_2-3) spin system, while irradiation at δ_H 4.26 (H-7, *dt*, J = 4.7; 9.3 Hz) revealed the connectivity of the (CH_3-17)-(CH-8)-(CH-7)-(CH_2-6)-(CH-5) entire system. The *α*-orientation for the 7-OH group was assigned based on NOE correlations (Fig. 2), which demonstrated interactions from the signal of H-7 with H-5 and H-8, indicating that these groups were *β*-co-oriented. Complete NMR data for compound **4** is given in Table 1.

The HRESIMS spectrum of the natural analogue **8** showed a protonated molecular ion at *m/z* 353.2334 $[M+H]^+$ (calcd. for $C_{20}H_{33}O_5$, 353.2328), together with a sodiated molecule ion at *m/z* 375.2144 $[M+Na]^+$ (calcd. for $C_{20}H_{32}O_5Na$, 375.2147), and also a potassiated molecule ion at *m/z* 391.1903 $[M+K]^+$ (calcd. for $C_{20}H_{32}O_5K$, 391.1887), which altogether allowed the molecular formula to be determined as $C_{20}H_{32}O_5$ and revealed the addition of two oxygen atoms to the substrate. A comparative inspection of the ^{1}H NMR spectrum from the oxidation product **8** with that of **1** [7] revealed the presence of new signals arising from the resonance of a typical methylene group having an adjacent *α,β*-unsaturated carbonyl system (δ_H 2.35; 1.92, *d*, J = 16.0 Hz), as well as the deshielding from the signal of H-1 from δ_H 5.37 to δ_H 5.79. It was also noticed, by comparison, the absence of the signal at δ_H 5.66 (H-14), together with the shielding of the signal assigned to CH_3-16 (from δ_H 2.10) to 1.18 ppm, suggesting that hydration of the side-chain double bond had occurred. The ^{13}C NMR spectrum showed a signal at δ_C 201.8, validating the presence of an *α,β*-unsaturated carbonyl system, and along with the DEPT-135 spectrum, the absence of the signals characteristic from the C—C 13,14-double bond was confirmed. The ^{1}J correlation between the singlet at δ_H 1.18 and the signal at δ_C 27.2 (both referent to CH_3-16) observed in the HSQC spectrum, in addition to ^{2}J correlations from δ_H 1.18 with δ_C 72.1 (C-13) and ^{3}J correlations with δ_C 37.6 (CH_2-12) and δ_C 48.3 (CH_2-14), reinforced the proposal of the side-chain double bond hydration. The TOCSY spectrum from the irradiation of the H-5 signal at δ_H 2.48 (dd, J = 4.4; 12.9 Hz) confirmed the connectivity from the groups belonging to the spin system consisting of (CH_3-17)-(CH-8)-(CH-7)-(CH_2-6)-(CH-5), contributing to the complete NMR assignments (Table 1) of

compound **8**. Key NOE correlations observed from NOESY experiments are given in Fig. 2. The hydroxyl group at C-13 was added by a formal conjugate addition of water to the α,β-unsaturated carboxyl side chain.

Fusarium species have been extensively used to perform modifications of diterpenoid substrates, including the hydroxylation of the tetracyclic diterpenoid isosteviol by *F. verticillioides*, producing its *ent*-7β-hydroxy and *ent*-12α-hydroxy derivatives[12]; the conversion of dehydroabietic acid into its 1α-hydroxy analogue by *F. oxysporum* and *F. moniliforme* [13]; hydroxylation of cupressic acid by *F. graminearum* to afford 3β,13-dihydroxy, 7α,13-dihydroxy, 8,13,17-trihydroxy, and 13,14,15-trihydroxy metabolites [14]; the hydroxyl functionalization of sclareol with *F. lini*, leading to the 1β-hydroxy and (12*S*)-12-hydroxy products [15]; the oxidation of *ent*-16-oxo-17-norkauran-19-oic acid into its 2β-hydroxy derivative, and kaurenoic acid into 1α-hydroxy analogue, both performed by *F. proliferatum* [16]; as well as oxidation of (+)-(5*S*, 8*S*, 9*R*, 10*S*)-labd-13-en-8β-ol-15-oic acid to its 7α-hydroxy derivative, and conversion of (+)-(4*R*, 5*S*, 8*R*, 9*S*)-hydroxy-*ent*-halima-1(10),13-(*E*)-dien-15-oic (**1**) acid into its 2-oxo product by *F. oxysporum* [7].

The transformation products 2β-hydroxy (**2**), 2-oxo (**3**), and 7α-hydroxy (**4**) formed with *F. oxysporum* in the present study are presumably associated with a P-450 cytochrome monooxygenase, an enzyme possibly responsible for promoting the substrate bio-hydroxylation, resulting in the activation of the C—H sp^3 bonds from positions C-2 and C-7. In this sense, the subsequent oxo-functionalization at C-2 was likely favored because of the higher reactivity of the C—H allylic bond than a secondary C—H sp^3 bond [7]. Cytochrome *P*-450 monooxygenases are Fe-heme containing enzymes, with a catalytically active intermediate [heme-Fe═O] that induces the removal of a substrate hydrogen atom (R-H) through a nonconcerted release of a radical (Ṙ), followed by the ready formation of the new hydroxyl bond (R-OH) [1,17].

In this investigation, we determined that while *M. verrucaria* showed specificity for positions C-2, C-18 and C-19, *F. oxysporum* promoted the selective oxidation of positions C-2 and C-7. Interestingly, both microorganisms demonstrated the ability for catalyzing C—H activation of the common position C-2 (**3**), however, a better yield was obtained with *F. oxysporum* (2.8%) than *M. verrucaria* (0.9%), which in turn provided a greater number of analogues.

Substrate modifications introduced by *R. similis* demonstrated a susceptible oxidation center in common with *F. oxysporum* and *M. verrucaria* (C-2), in contrast to a distinct oxy-reduction site corresponding to the C—C sp^2 bond from the aliphatic side-chain. Such transformations suggest C-2 oxo-functionalization through an oxidase-type enzyme, and the hydration of the 13,14-double bond intermediated by a hydratase [4,18].

The modifications described in this work contribute to emphasize the great potential that filamentous fungi offer as versatile catalysts for a range of reactions through their complex enzymatic machinery, as well as the susceptibility of diterpenoids as starting material since this biosynthetic class of metabolites is often endogenously produced by fungi [7].

2.2. Evaluation of cytotoxicity

It is well established in the literature that a number of halimane diterpenoids can display cytotoxic activities over a variety of cancer cell lines [19,9,20]. Therefore, metabolites **1** – **7** were evaluated for cytotoxic activity against HCT-116 (colon adenocarcinoma) and MCF-7 (breast adenocarcinoma) cell lines. However, all compounds were found to be inactive at the tested concentrations, indicating that oxy-functionalization of the inactive halimane substrate did not improve its bioactivity to these cancer cell lines. Some halimanes, such as (5*R*,8*R*,9*S*,13*R*)-halim-1,10-ene-15,16-diol, which contain non-functionalized rings and a distinct side chain, have shown activity against different cancer cell lines [21].

Table 2
MIC and MBC values of compound **1** against bacterial strains.

Bacterial strain	Main bacterial features	1	
		MIC (μg.ml^{-1})	MBC (μg.ml^{-1})
S. epidermidis ATCC 35984	Biofilm former	512	512
E. faecium VRE16	VRE_a	512	> 512
E. faecium VRE HBSJRP7	VRE_a, DapR	> 512	N.D.
E. faecium 1.1	Dap ss	> 512	N.D.
E. faecium 1.10	DapR	> 512	N.D.
S. aureus SA16	MRSA	512	512
S. aureus Mu50	MRSA, VISA	256	> 512
S. aureus SA88	MRSA, hDNSSA	512	> 512
S. aureus SA43 B2	MRSA	512	> 512
S. aureus SA43 B7	MRSA, TigR	512	> 512
S. aureus SA43	MRSA	512	> 512
S. aureus ATCC 25923		512	> 512
E. faecalis ATCC 29212		512	> 512
E. faecalis VRE109	VRE_a	512	> 512
E. faecalis VRE109 A42	VRE_a, TigR	512	512
E. faecalis VRE80	VRE_a, TigR	512	> 512
E. faecalis ATCC 700802 (V583)	VRE_b, GenR	256	> 512
A. baumannii ACI50		> 512	N.D.
K. pneumoniae ATCC 700603		> 512	N.D.
E. coli ATCC 25922		> 512	N.D.

MIC: Minimum inhibitory concentration.
MBC: Minimum bactericidal concentration.
N.D.: Not determined.
VRE: Vancomycin-Resistant Enterococci.
DapR: Daptomycin-Resistant.
Dap ss: Daptomycin - Super Sensitive.
MRSA: Methicillin-Resistant.
VISA: Vancomycin-Intermediate *Staphylococcus aureus*.
hDNSSA: heterogeneous Daptomycin-Non-Susceptible *Staphylococcus aureus*.
TigR: Tigecycline-Resistant.
GenR: Gentamicin-Resistant.

2.3. Antibacterial and biofilm reduction activities

Several studies highlight diterpenoids as a prominent class of compounds with antibacterial activity [9,19–22]. This biologically relevant activity, together with the need for new antibiotics to combat bacterial resistance [23], motivated us to investigate the antibacterial potential of substrate **1**.

Substrate **1** was screened for activity against bacteria of different species (Table 2), and displayed antibacterial effects against the Gram-positive bacteria *Staphylococcus epidermidis*, *Staphylococcus aureus*, *Enterococcus faecium* and *Enterococcus faecalis*. After determining some specific antibacterial potential of **1** against the aforementioned bacteria, this compound and its derivatives **2**, **3**, **4**, and **7** were assessed for their ability to reduce biofilm formed by *S. epidermidis* ATCC35984, a well-known biofilm-forming strain. Diterpenoid **1** was able to reduce biofilm with an effectiveness of 84 (± 6)%, at the concentration of 1.6 mM (Table 3), while its reduction values remained nearly constant under dilutions, at 1.2 and 0.8 mM, with 75 (± 12)% and 78 (± 11)% reduction, respectively, showing a moderate reduction ability at the lowest concentration tested. Derivatives **2** and **3** did not display any significant biofilm reduction capability, while metabolites **4** and **7** were able to weakly reduce biofilm formation, by 33 (± 21)% (**4**) and 61 (± 30)% (**7**), at 1.6 mM. The transformation products **5**, **6**, and **8** could not be assayed because the isolated amounts were not enough to enable reliable experiments to be performed.

3. Conclusion

The transformation of the diterpenoid substrate (**1**) by three filamentous fungi (*F. oxysporum*, *M. verrucaria*, and *R. similis*) provided

Table 3
Reduction values of compound **1** and derivatives **2**, **3**, **4**, and **7** on biofilm formed by *S. epidermidis* ATCC35984.

Compound	(% Reduction ± SEM) at 1.6 mM	(% Reduction ± SEM) at 1.2 mM	(% Reduction ± SEM) at 0.8 mM
1	84 ± 6	75 ± 12	78 ± 11
2	N.S.R.	N.D.	N.D.
3	N.S.R.	N.D.	N.D.
4	33 ± 21	N.D.	N.D.
7	61 ± 30	N.D.	N.D.

SEM: Standard error mean (n = 12).
N.D.: Not determined.
N.S.R.: Non-significant reduction ($p < 0.05$).

seven products, including four known compounds (**3**, **5**, **6**, and **7**) and three new derivatives (**2**, **4**, and **8**). The starting compound and its microbial oxidation products (**2–7**) were non-cytotoxic on HCT-116 and MCF-7 cancer cell lines at tested concentrations. On the other hand, compound **1** showed moderate reduction ability against the biofilm produced by *S. epidermidis* ATCC35984 (84% at 1.6 mM), while its derivatives **4** and **7** were only weakly active. These results emphasize the prominent potential of filamentous fungi associated with the microbiota of medicinal plants such as *Senna spectabilis* as versatile catalysts for performing very useful functionalization reactions through their complex enzymatic machinery, as well as the high susceptibility of halimane diterpenoids as microbial substrates.

4. Experimental

4.1. General experimental procedures

Specific rotations were determined on a PerkinElmer Model 341L Polarimeter (Shelton, CT, USA) with a quartz cell of 1 dm path length, at 25 °C. NMR experiments were performed on a Bruker AVANCE III HD spectrometer (14.1 T) with a Triple Inverse TCI CryoProbe head (5.0 mm), using chloroform-d_1 or methanol-d_4 both from Acros Organics (Morris, NJ, USA) as solvents. Chemical shifts (δ) were reported in ppm and coupling constants in Hertz (Hz). HRESIMS spectra were acquired on a micrOTOF-II mass spectrometer (Bruker Daltonics, Billerica, MA, USA), in negative or positive ion mode. Chromatographic analyses and purifications were carried out on a Shimadzu Prominence equipment (Kyoto, KY, Japan), using analytical (5 μm, C18, 100 Å, 150 × 4.60 mm) and semi-preparative (5 μm, C18, 100 Å, 250 × 4.60 mm) Phenomenex Kinetex® columns (Torrance, CA, USA).

4.2. Substrate and microorganisms

(+)-(4*R*, 5*S*, 8*R*, 9*S*)-18-Hydroxy-*ent*-halima-1(10),13-(*E*)-dien-15-oic acid (**1**) was isolated from the ethanolic extract of flowers of *Hymenaea stigonocarpa* (Fabaceae) following the procedure described by Monteiro and Co-workers [24] and identified by comparison of NMR spectroscopic data [7,24]. Plant material was collected in Brazilian Cerrado (Catalão, GO, Brazil) – voucher specimen GD 046, deposited in EMBRAPA Herbarium (Brasília, DF, Brazil).

Filamentous fungi strains - *Myrothecium verrucaria* (Cs-f23), *Fusarium oxysporum* (CSP-30) and *Rhinocladiella similis* (CSP-58) – were obtained from the NuBBE Collection – UNESP (Araraquara, SP, Brazil). *M. verrucaria*, an endophyte, was isolated from the leaves of *Senna spectabilis* (Fabaceae) [10], while both *F. oxysporum* and *R. similis* were obtained from the rhizosphere microbiota of the same plant species.

4.3. Biotransformation protocol

Fungi strains were grown in PDA (Potato Dextrose Agar) Petri dishes for 7 days, at 28 °C and then spores were used for liquid medium inoculation. The experimental conditions for achieving substrate oxidation were identical to those previously reported [7], except for incubation time and substrate concentration. In the first step, spore suspensions of each fungus were inoculated in 250 ml CZAPEK DOX broth, in two 500 ml flasks (pH ~ 5.3) and, incubated on a rotatory shaker at 110 rpm and 28 °C for 3 days. In the subsequent step, mycelia were submitted to filtration and resuspension in CZAPEK and then a solution of 100 mg substrate in 1 ml DMSO (dimethylsulfoxide) was administrated in each flask to afford a final concentration of 0.4 mg/ml prior to the reincubation under conditions specified in the first step. Substrate controls consisting of medium and substrate, and culture controls (medium and mycelium) were incubated in identical conditions.

Substrate and biotransformation products were monitored daily by analytical scale HPLC-DAD using 1 ml aliquots of each experiment.

4.4. Isolation of biotransformation products

At the end of the incubation period, the cultures were filtered in vacuo and the filtrate was successively extracted with ethyl acetate (1:1 v/v), three times. The organic layer was then separated and dried over anhydrous sodium sulfate before the solvent concentration under reduced pressure to provide the crude extracts. The individual extracts (replicates) were profiled and combined yielding the following amounts for posterior fractionation: *F. oxysporum* extract (FoE1) – 236.0 mg; *M. verrucaria* extract (MvE1) – 245.4 mg; and *R. similis* extract (RsE1) – 228.2 mg. The extracts were subjected to semi-preparative HPLC fractionation in linear gradient elution (25–90% acetonitrile 0.1% acidified formic acid, 35 min).

Separation of extract FoE1 resulted in 15 fractions, of which fraction FoE1.8 (R_t 15.80 – 16.25 min) provided compound **2** (0.8 mg, 1.6%), FoE1.6 (R_t 15.10 – 15.60 min) gave metabolite **3** (1.4 mg, 2.8%), and FoE1.10 (R_t 17.00 – 17.50 min) afforded bioproduct **4** (4.3 mg, 8.6%).

Extract MvE1 yielded 17 fractions, and fraction MvE1.4 (R_t 15.15 – 15.55 min) showed to be identical to that of compound **3** (0.9 mg, 1.8%), whilst MvE1.8 (R_t 21.20 – 21.65 min) afforded natural derivative **5** (1.0 mg, 2.0%), MvE1.16 (R_t 30.50 – 31.00 min) gave analogue **6** (4.4 mg, 8.8%) and, finally, MvE1.12 (R_t 25.00 – 25.50 min) provided compound **7** (5.4 mg, 10.8%).

RsE1 was chromatographed to generate 12 fractions, amongst which RsE1.5 (R_t 7.90 – 8.20 min) yielded compound **8** (1.0 mg, 2.0%).

(-)-(2*S**, 4*R**, 5*S**, 8*R**, 9*S**)-2,18-dihydroxy-*ent*-halima-1(10),13-(*E*)-dien-15-oic acid (**2**): white, amorphous solid, $[\alpha]_D^{25}$ − 1.4 (*c* 0.07, MeOH); ^{1}H and ^{13}C NMR data, see Table 1, HRESIMS *m/z* 335.2236 $[M-H]^-$ (calcd. for $C_{20}H_{31}O_4$ 335.2228).

(+)-(4*R**, 5*S**, 7*S**, 8*S**, 9*S**)-7,18-dihydroxy-*ent*-halima-1(10),13-(*E*)-dien-15-oic acid (**4**): white, amorphous solid, $[\alpha]_D^{25}$ + 99,6 (*c* 0.09, MeOH); ^{1}H and ^{13}C NMR data, see Table 1; HRESIMS *m/z* 335,2223 $[M-H]^-$ (calcd. for $C_{20}H_{31}O_4$ 335,2228).

(+)-(4*R**, 5*S**, 8*R**, 9*S**)-13,18-dihydroxy-*ent*-halima-1(10)-(*E*)-en-15-oic acid (**8**): white, amorphous solid, $[\alpha]_D^{25}$ + 20,0 (*c* 0.1, MeOH); ^{1}H and ^{13}C NMR data, see Table 1; HRESIMS: *m/z* 353.2334 $[M+H]^+$ (calcd. for $C_{20}H_{33}O_5$ 353.2328) and *m/z* 375.2144 $[M+Na]^+$ (calcd. for $C_{20}H_{32}O_5Na$ 375.2147)

4.5. Cytotoxicity evaluation through MTT assay

Cytotoxic activity was assessed against two human cancer cell lines obtained from *American Type Culture Collection* (Manassas, Virginia, EUA) – colon adenocarcinoma (HCT-116, ATCC® CCL-247™) and breast adenocarcinoma (MCF-7, ATCC® HTB-22). Cells were suspended in RPMI 1640 medium supplemented with 10% fetal bovine serum (v/v), and 1% penicillin/streptomycin, at 37 °C under 5% CO_2 atmosphere, to give a final concentration 1×10^4 cells per 200 μl medium in each well of the culture plate. After 24 h of incubation, samples of compounds **1** –

7 dissolved in DMSO were added to the suspension at concentrations of 5.0 and 50.0 μM (duplicate) and reincubated for 72 hrs. The antiproliferative effect of compounds was evaluated *in vitro* by MTT [3-(4,5-dimethyl-2-thiazolyl)- 2,5-diphenyl-2*H*-tetrazolium bromide] assay [25]. Doxorubicin (0.003–10 μM) Sigma Aldrich – St. Louis, MO, USA) was applied as a positive control and DMSO (Labsynth - Diadema, SP, Brazil) as a negative control. Mean inhibitory values were calculated by non-linear regression using the software GraphPad Prism 5.0.

4.6. Evaluation of antibacterial activity

Minimum inhibitory concentration (MIC) values were determined according to the recommendations of the Clinical and Laboratory Standards Institute (CLSI) [26]. Antibacterial assay was performed through the microdilution method. A sample of the compound **1** was initially screened against Gram-positive bacterial strains (*Staphylococcus epidermidis* ATCC 35984; *Staphylococcus aureus* ATCC 25923; *Enterococcus faecalis* ATCC 29212; and *Enterococcus faecium* VRE16) and Gram-negative strains (*Klebsiella pneumoniae* ATCC 700603; and *Escherichia coli* ATCC 25922). A stock solution of the compound was made in DMSO. This solution was diluted in Mueller Hinton Cation Adjusted (MHCA) broth covering a concentration range from 512 $\mu g.ml^{-1}$ to 0.06 $\mu g.ml^{-1}$at final concentration of 1% DMSO. The bacteria cell suspension was incubated (5×10^5 $CFU.ml^{-1}$, duplicate) with the compound for 24 h, at 37 °C. The microtiter plates were then analyzed by visual reading. Bacterial suspensions in MHCA broth and 1% DMSO were used as positive control while negative controls consisted of only sterile broth. Following the activity detected in the aforementioned preliminary screening, compound **1** was evaluated against a panel of Gram-positive multidrug-resistant (MDR) bacteria according to the same procedure.

The minimal bactericidal concentration (MBC) was evaluated for inhibited bacterial growth on MIC plate assay. MBC was determined using 100 μl suspension from each well by sub-culturing on MHCA agar plates for 24 h, at 37 °C. MBC was defined as the lowest compound concentration at which no bacterial growth was visualized. For the determination of activity, the compounds that had MBC/MIC ratio lower than or equal to 4 were considered bactericidal, above this value the compound activity was considered bacteriostatic [27].

4.7. Biofilm reduction assay

Biofilm reduction abilities of compounds **1**, **2**, **3**, **4**, and **7** were assessed using *S. epidermidis* ATCC 35984, a well-known biofilm-forming strain. This strain and *S. epidermidis* ATCC 12228, a biofilm-negative strain, were used in the assay as positive and negative controls, respectively. All compounds were tested at a concentration of 1.6 mM, equivalent to 512 $\mu g.ml^{-1}$ for compound **1**. The strains were pre-cultured in 35 ml Brain Heart Infusion (BHI) broth supplemented with 0.75% glucose (*w/v*) overnight at 37°C. Cultures were adjusted as already described [28]. Aliquots of 200 μl bacterial suspensions were statically incubated in polystyrene 96-well flat-bottom microplates at 37 °C for 24 h to propitiate bacterial adhesion. After the removal of planktonic cells, the wells were washed three times with phosphate-buffered saline (PBS; pH = 7.4), and cells were subsequently incubated for additional 24 h, at 37 °C, in the presence of fresh medium for positive and negative controls and fresh medium plus compounds at 1.6 mM in the wells with the biofilm forming strain [29]. In the next stage, cells were washed and subjected to crystal violet staining (0.2% *w/v*) and examined in a microplate reader at 600 nm as previously described [28]. A comparison between *S. epidermidis* ATCC 12,228 and *S. epidermidis* ATCC 35,984 used as controls were made with two-tailed Student's T-test ($p < 0.05$) to make sure biofilm formation succeeded. One-way analysis of variance (ANOVA) was used to compare the absorbance values of treated and non-treated *S. epidermidis* ATCC 35,984 to access biofilm reduction ($p < 0.05$). All experiments were performed in 12 replicates.

Acknowledgments

The authors are grateful to Professor I. R. Nascimento from UNESP - IQAr and to M.Sc. C. L. Cunha for optical rotation measurements.

Author Contributions

A.F.M. conceived the idea, obtained the biotransformation results, and draft the manuscript; G.M.R performed the antibacterial and biofilm reduction assays; L.V.S. conducted the biotransformation experiments with *R. similis* and its bioproduct isolation; L.A.C. assessed the cytotoxic activity of substrate and bioproducts; L.V.C-L. directed the cytotoxic assays; I.L.B.C.C. directed the antibacterial and biofilm assays; I. C-G. directed the study and revised the manuscript.

Competing interests

The authors declare no competing interests.

Funding Sources

This work was funded by grants from Coordenação de Aperfeiçoamento de Pessoal de Nível Superior - CAPES (PROEX – 1427484; Finance code 001) and Fundação de Amparo à Pesquisa do Estado de São Paulo (FAPESP) through CEPID Program - CIBFar Project (2013/07600-3; 2016/24969-9). Additional research grant awarded to I. C. G. (449523/2014-4) and the National Institute of Science and Technology - INCT BioNat, grant # 465637/ 2014-0, funded by Conselho Nacional de Desenvolvimento Científico e Tecnológico (CNPq) is also acknowledged.

Appendix A. Supplementary material

Supplementary data to this article can be found online at https://doi.org/10.1016/j.bioorg.2019.02.021.

References

[1] A. Ilie, R. Agudo, G.-D. Roiban, M.T. Reetz, P450-catalyzed regio- and stereoselective oxidative hydroxylation of disubstituted cyclohexanes creation of three centers of chirality in a single CH-activation event, Tetrahedron 71 (3) (2015) 470–475.
[2] T. Gensch, M.N. Hopkinson, F. Glorius, J. Wencel-Delord, Mild metal-catalyzed C-H activation: examples and concepts, Chem. Soc. Rev. 45 (10) (2016) 2900–2936.
[3] J. Latham, J.-M. Henry, H.H. Sharif, B.R.K. Menon, S.A. Shepherd, M.F. Greaney, J. Micklefield, Integrated catalysis opens new arylation pathways via regiodivergent enzymatic C-H activation, Nat. Commun. 7 (2016) 11873.
[4] M. Schrewe, M.K. Julsing, B. Buhler, A. Schmid, Whole-cell biocatalysis for selective and productive C-O functional group introduction and modification, Chem. Soc. Rev. 42 (15) (2013) 6346–6377.
[5] S.-H. Xu, W.-W. Wang, C. Zhang, X.-F. Liu, B.-Y. Yu, J. Zhang, Site-selective oxidation of unactivated C-H sp3 bonds of oleanane triterpenes by *Streptomyces griseus* ATCC 13273, Tetrahedron 73 (21) (2017) 3086–3092.
[6] C.M. Clouthier, J.N. Pelletier, Expanding the organic toolbox: a guide to integrating biocatalysis in synthesis, Chem. Soc. Rev. 41 (4) (2012) 1585–1605.
[7] A.F. Monteiro, C. Seidl, V.G.P. Severino, C.L. Cardoso, I. Castro-Gamboa, Biotransformation of labdane and halimane diterpenoids by two filamentous fungi strains, R. Soc. Open Sci. 4 (11) (2017).
[8] A. Ludwiczuk, K. Skalicka-Woźniak, M.I. Georgiev, Chapter 11 - Terpenoids A2 - Badal, Simone, in: R. Delgoda (Ed.), Pharmacognosy, Academic Press, Boston, 2017, pp. 233–266.
[9] A.M. Roncero, I.E. Tobal, R.F. Moro, D. Díez, I.S. Marcos, Halimane diterpenoids: sources, structures, nomenclature and biological activities, Nat. Prod. Rep. (2018).
[10] D.M. Selegato, A.F. Monteiro, N.C. Vieira, P. Cardoso, V.D. Pavani, V.S. Bolzani, I. Castro-Gamboa, Update: Biological and Chemical Aspects of *Senna spectabilis*, J. Braz. Chem. Soc. 28 (3) (2017) 415–426.
[11] A.F. Monteiro, Perfil metabólico das raízes de Senna spectabilis e exploração de fungos associados à sua microbiota para produção e biotransformação de metabólitos secundários, Universidade Estadual Paulista (UNESP).
[12] B.H. de Oliveira, R.A. Strapasson, Biotransformation of isosteviol by *Fusarium verticilloides*, Phytochemistry 43 (2) (1996) 393–395.
[13] A.A. Tapia, M.D. Vallejo, S.C. Gouiric, G.E. Feresin, P.C. Rossomando, D.A. Bustos, Hydroxylation of dehydroabietic acid by *Fusarium* species, Phytochemistry 46 (1) (1997) 131–133.

[14] E. Rodrigues-Filho, R.F. Magnani, W. Xie, C.J. Mirocha, S.V. Pathre, Hydroxylation of the labdane diterpene cupressic acid by *Fusarium graminearum*, J. Braz. Chem. Soc. 13 (2002) 266–269.
[15] M.I. Choudhary, Z.A. Siddiqui, S. Hussain, R. Atta ur, Structure elucidation and antibacterial activity of new fungal metabolites of sclareol, Chem. Biodivers. 3 (1) (2006) 54–61.
[16] A.D. Rocha, H.D.S. Vieira, J.A. Takahashi, M.A.D. Boaventura, Synthesis of a new allelopathic agent from the biotransformation of ent-15α-hydroxy-16-kauren-19-oic acid with *Fusarium proliferatum*, Nat. Prod. Res. 31 (22) (2017) 2647–2653.
[17] P.R. Ortiz de Montellano, Cytochrome P450: Structure, Mechanism, and Biochemistry, 3rd ed., Springer, Berlin, Germany, 2005.
[18] V. Resch, U. Hanefeld, The selective addition of water, Catal. Sci. Technol. 5 (3) (2015) 1385–1399.
[19] M. Rico-Martinez, F.G. Medina, J.G. Marrero, S. Osegueda-Robles, Biotransformation of diterpenes, RSC Adv. 4 (21) (2014) 10627–10647.
[20] L.M.T. Frija, R.F.M. Frade, C.A.M. Afonso, Isolation, chemical, and biotransformation routes of labdane-type diterpenes, Chem. Rev. 111 (8) (2011) 4418–4452.
[21] C.G. Silva, H.M. Santos Júnior, J.P. Barbosa, G.L. Costa, F.A.R. Rodrigues, D.F. Oliveira, L.V. Costa-Lotufo, R.J.V. Alves, E.C.A. Eleutherio, C.M. Rezende, Structure elucidation, antimicrobial and cytotoxic activities of a halimane isolated from *Vellozia kolbekii* Alves (Velloziaceae), Chem. Biodivers. 12 (12) (2015) 1891–1901.
[22] T.S. Porto, N.A.J.C. Furtado, V.C.G. Heleno, C.H.G. Martins, F.B. Da Costa, M.E. Severiano, A.N. Silva, R.C.S. Veneziani, S.R. Ambrósio, Antimicrobial ent-pimarane diterpenes from *Viguiera arenaria* against Gram-positive bacteria, Fitoterapia 80 (7) (2009) 432–436.
[23] E. Martens, A.L. Demain, The antibiotic resistance crisis, with a focus on the United States, J. Antibiot. 70 (2017) 520.
[24] A.F. Monteiro, J.M. Batista Jr., M.A. Machado, R.P. Severino, E.W. Blanch, V.S. Bolzani, P.C. Vieira, V.G.P. Severino, Structure and absolute configuration of diterpenoids from *Hymenaea stigonocarpa*, J. Nat. Prod. 78 (6) (2015) 1451–1455.
[25] T. Mosmann, Rapid colorimetric assay for cellular growth and survival: Application to proliferation and cytotoxicity assays, J. Immunol. Methods 65 (1–2) (1983) 55–63.
[26] Clinical and Laboratory Standards Institute (CLSI). Performance Standards for Antimicrobial Susceptibility Testing; 33th Informational Supplement; CLSI Document m100-s24; Clinical and Laboratory Standards Institute: Wayne, PA, USA, 2014; Volume 34.
[27] G.A. Pankey, L.D. Sabath, Clinical relevance of bacteriostatic versus bactericidal mechanisms of action in the treatment of gram-positive bacterial infections, Clin. Infect. Dis. 38 (6) (2004) 864–870.
[28] D. Davies, Understanding biofilm resistance to antibacterial agents, Nat. Rev. Drug Discovery 2 (2) (2003) 114–122.
[29] N. Qin, X. Tan, Y. Jiao, L. Liu, W. Zhao, S. Yang, A. Jia, RNA-Seq-based transcriptome analysis of methicillin-resistant *Staphylococcus aureus* biofilm inhibition by ursolic acid and resveratrol, Sci. Rep. 4 (2014) 5467.